

Supplemental Materials for

Tandem CAR-T cells targeting FOLR1 and MSLN enhance the antitumor effects in ovarian cancer.

Zhen Liang^{1, #}, Jiao Dong^{1, 2, #}, Neng Yang¹, Si-Di Li¹, Ze-Yu Yang³, Rui Huang⁴,
Feng-Jie Li¹, Wen-Ting Wang¹, Jia-Kui Ren¹, Jie Lei⁵, Chen Xu⁶, Dan Wang¹,
Yan-Zhou Wang¹, Zhi-Qing Liang^{1, *}

¹ Department of Obstetrics and Gynecology, Southwest Hospital, Army Medical University (Third Military Medical University), Chongqing, China.

² Department of Obstetrics and Gynecology, Guangyuan Traditional Chinese Medicine Hospital, Guangyuan, China.

³ Breast and Thyroid Surgical Department, Chongqing General Hospital, University of Chinese Academy of Sciences, Chongqing, China.

⁴ Institute of Pathology and Southwest Cancer Center, Southwest Hospital, Army Medical University (Third Military Medical University), Chongqing, China.

⁵ Department of Internal Medicine, Hui Long-Ba Town Hospital, Chongqing, China.

⁶ Department of Hepatobiliary Surgery, Xijing Hospital, The Fourth Military Medical University, Xi'an, China.

These authors contributed equally to the work.

Declarations of interest: none

***Corresponding author:**

Dr. Zhi-Qing Liang, Ph.D.

Professor

Department of Obstetrics and Gynecology,

24 Southwest Hospital,
25 Army Medical University (Third Military Medical University),
26 30 Gaotanyan Main Street, Shapingba, Chongqing, China 400038
27 Phone: +86-23-68765401
28 ORCID: 0000-0001-6459-2541
29 E-mail: lzq@tmmu.edu.cn, zhilzliang@outlook.com, or zhilzliang@163.com

30 **This file includes the following:**

31 Methods

32 Supplemental Tables 1 to 5

33 Supplemental Figures 1 to 4

34 **Methods**

35 **Identification of upregulated genes from the GEO database**

36 We processed the downloaded files with RStudio software (3.5.3 version, Vienna,
37 Austria) and then standardized, calibrated, and log 2 converted the resulting data. The
38 cutoff criteria for upregulated gene screening were $p < 0.01$ and $|\log FC| \geq 2$. The
39 coexpressed upregulated genes in these four gene expression profiles were evaluated
40 by Venn diagram analysis. After the coexpressed upregulated genes were identified,
41 cluster analysis was performed by RStudio software with a heatmap package
42 (heatmap) to further reveal significant differences between the normal and OV tissues.
43 The volcano plot of these four gene expression profiles was generated with R
44 software, and the criteria $p < 0.01$ and $|\log FC| \geq 2$ were used.

45 **Immunohistochemistry (IHC) staining and quantification**

46 In brief, tissue slides were heated and deparaffinized in xylene immediately.
47 After rehydration in a graded series of ethanol solutions, tissue slides were submerged
48 in citrate antigen retrieval solution (pH=6.0) and heated in a microwave oven for
49 antigen retrieval, and the activity of endogenous peroxidases was blocked by
50 hydrogen peroxide. Subsequently, the sections were incubated with an anti-FOLR1
51 rabbit polyclonal antibody (Abcam, 1:100 dilution) and anti-MSLN mouse
52 monoclonal antibody (Invitrogen, 1:10 dilution) overnight at 4°C. Negative IHC
53 staining controls obtained by omitting the primary antibodies were routinely used.
54 After washing, the slides were incubated with corresponding secondary antibodies
55 (ZSGB-BIO, China), stained with diaminobenzidine (DAB; DAKO, S196130-2,

56 Denmark). Finally, the samples were counterstained with hematoxylin and
57 dehydrated.

58 The IHC staining was scored from 0 to 3 (representing negative, weak, moderate,
59 and strong staining, respectively). Based on the percentage of positive tumor cells
60 observed per tissue, the extent of IHC staining was scored: 1 (0-25%), 2 (26-50%), 3
61 (51-75%), and 4 (76-100%). The final staining index (0-12) of each sample was
62 obtained from the multiplying results of two scores. High and low expression was
63 defined as a final score of 6-12 and 0-4, respectively. Alternatively, using integrated
64 optical density (IOD) analyzed with Image-Pro® Plus software (version 6.0; Media
65 Cybernetics, Inc.) to show the quantitative analysis results.

66 **Cells lines**

67 The HEK293T cell lines and human OV cell lines SNU119, SKOV3, and A2780
68 were obtained from the Type Culture Collection of the Chinese Academy of Sciences
69 (Shanghai, China). These cells were cultured in RPMI-1640 medium or DMEM
70 supplemented with 10% fetal bovine serum (FBS, HyClone or Gibco), 100 µg/ml
71 penicillin, and 100 U/ml streptomycin (Invitrogen). SNU119, SKOV3, and A2780
72 target cells were transduced with a lentiviral vector encoding the firefly luciferase
73 gene to generate SNU119-Luc, SKOV-3-Luc, and A2780-Luc cells.

74 **Lentiviral vector production and CAR-T Cell production**

75 Plasmids were cotransfected with the packaging plasmids psPAX2 and pMD2.G

76 (ratio 2.5:2:1) into HEK293T cells. Supernatants containing viral particles were
77 collected at 24 and 48 hours after transfection, pooled, filtered, concentrated by a
78 Lenti-X concentrator (Clontech), resuspended in PBS supplemented with 1% FBS,
79 aliquoted, and used immediately or stored at -80°C. Viral titers were measured by
80 flow cytometry (FC) with serial dilutions.

81 CD3⁺ T cells were isolated from peripheral blood mononuclear cells (PBMCs,
82 StemCell Technologies) using an EasySep human T cell isolation kit (StemCell
83 Technologies) and cultured in RPMI 1640 medium supplemented with 10% FBS
84 (Gibco), 0.1 mg/mL streptomycin (Gibco), 100 U/mL penicillin (Gibco), 2 mM
85 L-glutamine (Gibco), and 100 IU/ml recombinant human IL-2 (Miltenyi Biotec). T
86 cells were activated by Human CD3/CD28 T Cell Activator (Stem Cell Technologies)
87 for 24 hours and infected with lentiviruses containing the different CAR transgenes in
88 RetroNectin-coated (Takara, 32 µg/mL) 24-well plates at a multiplicity of infection
89 (MOI) of 10. The T cells were spin-infected at 2,000 g for 2 hours with the virus at
90 32°C. After transduction, the cells were cultured in T cell medium containing 100 U
91 of IL-2 per ml and expanded for approximately 10 days. Activated T cells were
92 cultured at concentrations between 0.5 and 1 × 10⁶ cells/mL.

93 **Flow cytometry analysis**

94 Up to 10⁶ cells were stained with fluorochrome-conjugated antibodies for 30 min
95 at 4°C in the dark. T cells were stained with an APC-conjugated anti-F(ab')₂ antibody
96 (Jackson ImmunoResearch) to determine the expression of the desired CAR transgene.

97 FOLR1 and MSLN expression in tumor cell lines was detected with a PE-conjugated
98 anti-FOLR1 antibody (BioLegend) and an APC-conjugated anti-MSLN antibody
99 (*R&D Systems*). T cell surface molecules were stained with anti-human CD3
100 (PerCP-Cy5.5, BD), CD4 (APC-Cy7, BioLegend), CD8 (FITC, BD), CD62L (PE,
101 BioLegend), and CD45RO (APC, BD) antibodies. The phenotype of CAR-T cells was
102 determined by evaluating the percentages of CD62L⁺CD45RO⁺ central memory T
103 cells (T_{cm}) and CD62L⁻CD45RO⁺ effector T cells (T_{em}) after 48 h of coculture with
104 SNU119 cells. The non-transduced T cells were treated equally and served as
105 Control-T cells. Fluorescence was analyzed using a BD FACSCanto flow cytometer,
106 and data were analyzed using FlowJo V10 software.

107 **Cytokine Release and cell proliferation assays**

108 Cytokine production was detected by intracellular cytokine staining of T cells.
109 CAR-T cells were incubated with SNU119 cells at an effector-to-target (E:T) cell ratio
110 of 2:1 in 200 µL of complete medium (without IL-2) and then incubated with Golgi
111 Plug to block exocytosis of cytokines for 4 h (BD Biosciences). Following this, the
112 cells were stained for surface markers (CD3/APC, CD4/APC-Cy7, and CD8/FITC),
113 followed by fixation, permeabilization, and staining for intracellular proteins with the
114 Cytofix/Cytoperm Fixation/Permeabilization Solution Kit (BD Biosciences).
115 Intracellular cytokine staining was performed with PE/Cy7-conjugated anti-human
116 IFN- γ , PE-conjugated anti-human TNF- α , PerCP-Cy5.5-conjugated anti-human IL-12,
117 and BV421-conjugated anti-human IL-2 antibodies (BioLegend). For the proliferation

118 assay, T cells (1×10^6) were plated in 6-well plates (without IL-2) and stimulated
119 weekly with SNU119 cells at an E:T ratio of 1:1. Cell numbers and size were
120 evaluated using a Bio-Rad TC20™ cell counter (USA). For the degranulation assay,
121 CAR-T cells were cocultured with SNU119 cells at an E:T ratio of 1:1 in complete
122 medium containing the anti-human perforin-PerCP-Cy5.5 and anti-human granzyme
123 B-Pacific Blue antibody (BioLegend) for 1 h, followed by incubation with a Golgi
124 Plug (BD Biosciences) for 3 h.

125 **Cytotoxicity assay**

126 CAR-T cells were cocultured with human ovarian cell lines with different
127 expression levels of FOLR1 and MSLN at different ratios for 18 hours to assess
128 cytotoxicity and maintain a total cell concentration of 1×10^6 /mL. The amount of
129 lactate dehydrogenase (LDH) in the supernatant was quantified using a CytoTox 96®
130 Non-Radioactive Cytotoxicity Assay kit (Promega). The percent specific killing of
131 target cells (lytic activity) was calculated according to the manufacturer's instructions
132 based on absorbance values (490 nm) subtracted from the culture medium background.
133 Calculations for % cell lysis were consisted with previously described [1].

134 **Xenograft mouse model**

135 For *in vivo* study of CAR-T cell functions, 6- to 8-week-old female
136 NOD-*Prkdc*^{scid}*IL2rg*^{tm1}/Bcgen (B-NDG, Biocytogen) mice were subcutaneously
137 injected with 5×10^6 SNU119-luciferase cells in the left groin. Approximately 10 days
138 later, the tumor volume reached approximately 50 to 100 mm³. The tumor-bearing

139 mice were randomly assigned into 4 groups and were injected i.v. with 1×10^7
140 untransfected (Control-T), FOLR1-CAR, MSLN-CAR, or Tandem-CAR T cells in
141 200 μ l of PBS. An IVIS imaging platform with Living Image software (PerkinElmer)
142 was used to evaluate the bioluminescence imaging (BLI) and BLI data was given as
143 the average flux (photons per second/area[mm^2]). Additionally, tumor volume was
144 measured every three days and calculated based on the equation: length \times (width)² \times
145 0.5. Tumor BLI was performed until death or sacrifice when tissues were harvested
146 for analysis. Mice were euthanized when maximum tumor diameters exceeded 2 cm
147 or bodyweight loss over 20%. We collected peripheral blood samples when mice were
148 sacrificed, red blood cells were lysed using AR1118 Lysing Buffer (Boster Biological
149 Technology), and the remaining cells were stained with an APC-conjugated anti-CD3
150 antibody for FC. To analyze the intratumoral infiltration of T cells, IHC staining was
151 performed using standard procedures. The expression of FOLR1 and MSLN in the
152 different groups was also determined by IHC staining. Primary rabbit anti-human
153 CD3 ϵ (CST), rabbit anti-human FOLR1 (Abcam) and mouse anti-human MSLN
154 antibodies (Invitrogen) and a biotinylated secondary goat anti-rabbit/mouse antibody
155 were used.

156

Table S1. Characteristics of the GEO microarray datasets

157

Chip serial number	OV patients	Normal patients	Platform
GSE28721	8	2	GPL6884 Illumina HumanWG-6 v3.0 expression beadchip GPL6947 Illumina HumanHT-12 V3.0 expression beadchip
GSE66957	57	12	GPL15048 Rosetta/Merck Human RSTA Custom Affymetrix 2.0 microarray
GSE36668	4	4	GPL570 [HG-U133_Plus_2] Affymetrix Human Genome U133 Plus 2.0 Array
GSE4122	32	14	GPL201 [HG-Focus] Affymetrix Human HG-Focus Target Array

158 **Table S2. Descriptive statistics for clinic-pathological features in ovarian cancer**
 159 **patients**

Variable	Number of patients	Percentage (%)
Age		
≤50	77	48.13
>50	83	51.87
Histological subtypes		
Serous	100	62.50
Mucinous	33	20.62
Endometrioid	17	10.63
Others ^a	10	6.25
Grade of differentiation		
1	19	12.03
2	35	22.15
3	104	65.82
FIGO stage		
I	9	5.70
II	37	23.42
III	79	50.00
IV	33	20.88
Lymph node metastasis		
Positive	42	26.58
Negative	116	73.42
Progression status		
No recurrence	31	19.62
Recurred	127	80.38

160 ^a Malignant Brenner tumor, 1 case; Clear-cell, 3 cases; Borderline mucinous tumor, 2 cases; Squamous
 161 cell carcinoma, 2 cases; Yolk sac tumor, 2 cases.

Table S3. Association between FOLR1 and MSLN expression and clinic-pathological criteria

Variable	FOLR1 expression (n=160)			MSLN expression (n=160)		
	High	Low	<i>P</i> value	High	Low	<i>P</i> value
Age			0.791			0.198
≤50	58 (36.25%)	19 (11.87%)		33 (5%)	44 (43.13%)	
>50	64 (40.00%)	19 (11.88%)		44 (11.25%)	39 (40.62%)	
Histological subtypes			0.178			0.048*
Serous	76 (47.50%)	24 (15.00%)		58 (13.75%)	42 (48.75%)	
Mucinous	22 (13.75%)	11 (6.88%)		9 (0.62%)	24 (20.00%)	
Endometrioid	16 (10.00%)	1 (0.62%)		8 (1.25%)	9 (9.38%)	
Others ^a	8 (5.00%)	2 (1.25%)		2 (0.62%)	8 (5.63%)	
Grade of differentiation			0.515			0.507
1-2	43 (27.22%)	11 (6.96%)		24 (3.17%)	30 (31.01%)	
3	78 (49.37%)	26 (16.45%)		52 (12.66%)	52 (53.16%)	
FIGO stage			0.048*			7.518E-05*
I-II	40 (25.32%)	6 (3.80%)		16 (0.0%)	30 (29.11%)	
III-IV	81 (51.26%)	31 (19.62%)		60 (15.82%)	52 (55.06%)	
Lymph node metastasis			0.178			0.008*
Positive	29 (18.35%)	13 (8.23%)		24 (7.59%)	18 (18.99%)	
Negative	92 (58.23%)	24 (15.19%)		52 (8.23%)	64 (65.19%)	
Progression status			0.285			0.062
No recurrence	26 (16.45%)	5 (3.17)		9 (0.63%)	22 (18.99%)	
Recurred	95 (60.13%)	32 (20.25%)		67 (15.19%)	60 (65.19%)	
Survival status			0.001*			0.007*
Living	66 (41.25%)	9 (5.63%)		32 (3.75%)	43 (43.12%)	
Dead	56 (35.00%)	29 (18.12%)		45 (12.50%)	40 (40.63%)	

163 ^a Malignant Brenner tumor, 1 case; Clear-cell, 3 cases; Borderline mucinous tumor, 2 cases; Squamous cell carcinoma, 2 cases; Yolk sac tumor, 2 cases.

Table S4. Univariate and multivariate analyses of different prognostic parameters

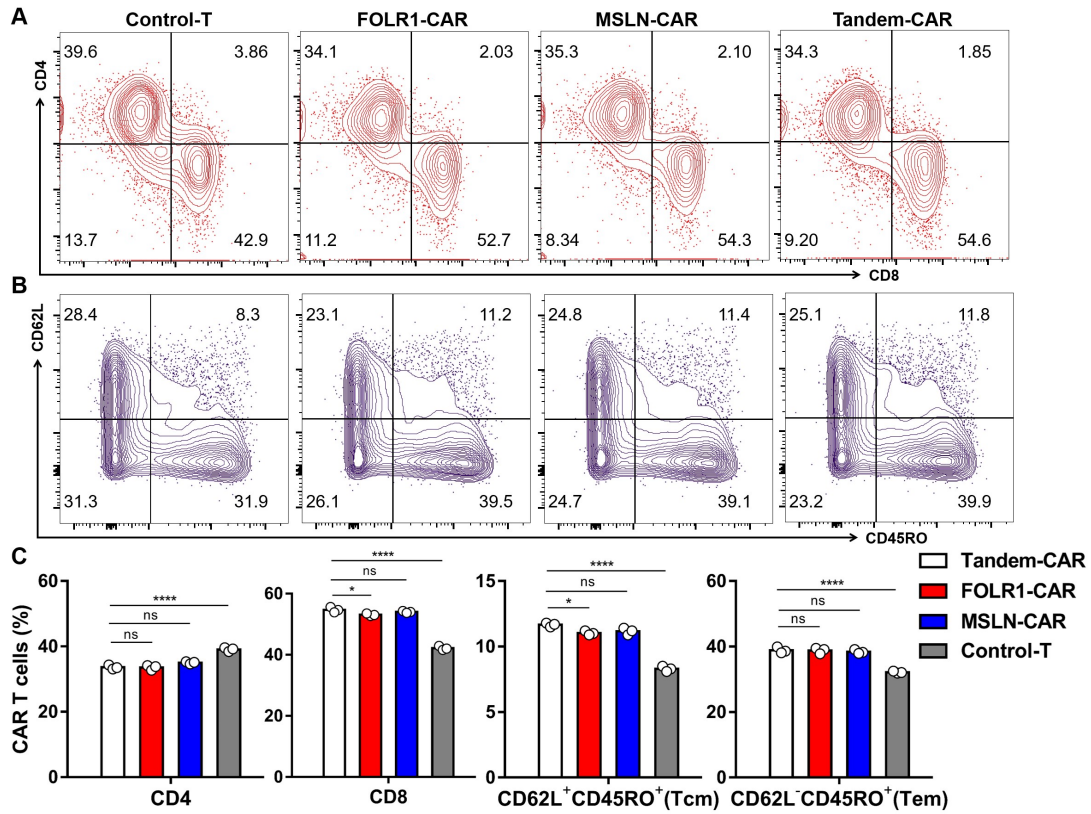
Variable	Case	Univariate analysis				Multivariate analysis			
		OS(M)		DFS(M)		OS(M)		DFS(M)	
		OS(M)	<i>P</i>	DFS(M)	<i>P</i>	HR (95% CI)	<i>P</i>	HR (95% CI)	<i>P</i>
Age at Diagnosis			0.082		0.031*		0.343		0.460
≤50	77	62.91		50.14		1.0		1.0	
>50	83	54.58		36.72		1.251 (0.788-1.986)		0.864 (0.587-1.273)	
Histological subtypes			0.000*		0.000*		0.032*		0.078
Serous	100	51.09		36.45		1.0		1.0	
Non-serous ^a	60	71.08		54.40		0.553 (0.321-0.950)		0.700 (0.472-1.040)	
Grade			0.003*		0.005*		0.128		0.026*
1-2	54	64.43		49.06		1.0		1.0	
3	104	54.73		39.01		1.556 (0.880-2.749)		1.693 (1.065-2.693)	
FIGO stage			0.000*		0.000*		0.000*		0.000*
I-II	46	79.80		68.80		1.0		1.0	
III-IV	112	49.11		31.62		12.111 (4.128-35.536)		6.652 (3.620-12.224)	
Lymph-node metastasis			0.000*		0.000*		0.000*		0.001*
Negative	116	67.98		50.40		1.0		1.0	
Positive	42	30.60		20.48		3.245 (1.981-5.315)		2.042 (1.327-3.141)	
FOLR1 Expression			0.004*		0.0078*		0.047*		0.697
FOLR1 ^{low}	38	49.05		37.47		1.0		1.0	
FOLR1 ^{high}	122	61.56		44.96		0.564 (0.321-0.991)		0.918 (0.596-1.414)	
MSLN Expression			0.008*		0.0057*		0.505		0.353
MSLN ^{low}	134	60.39		45.09		1.0		1.0	
MSLN ^{high}	26	49.31		33.35		1.228 (0.672-2.246)		1.268 (0.769-2.091)	

165 ^a Mucinous, 33 cases; Endometrioid, 17 cases; Malignant Brenner tumor, 1 case; Clear-cell, 3 cases; Borderline mucinous tumor, 2 cases; Squamous cell carcinoma, 2 cases;

166 Yolk sac tumor, 2 cases.

167 **Table S5. The relevance expression of FOLR1 and MSLN in ovarian cancer as**
 168 **judged by immunocytochemistry**

MSLN expression (n=160)	FOLR1 expression (n=160)		
	Positive	Negative	Total
Positive	57 (35.63%)	20 (12.50%)	77
Negative	65 (40.63%)	57 (35.62%)	122



169

170 **Figure S1. Phenotype of Tandem-CAR T cells compared to that of single-target CAR-T cells.**

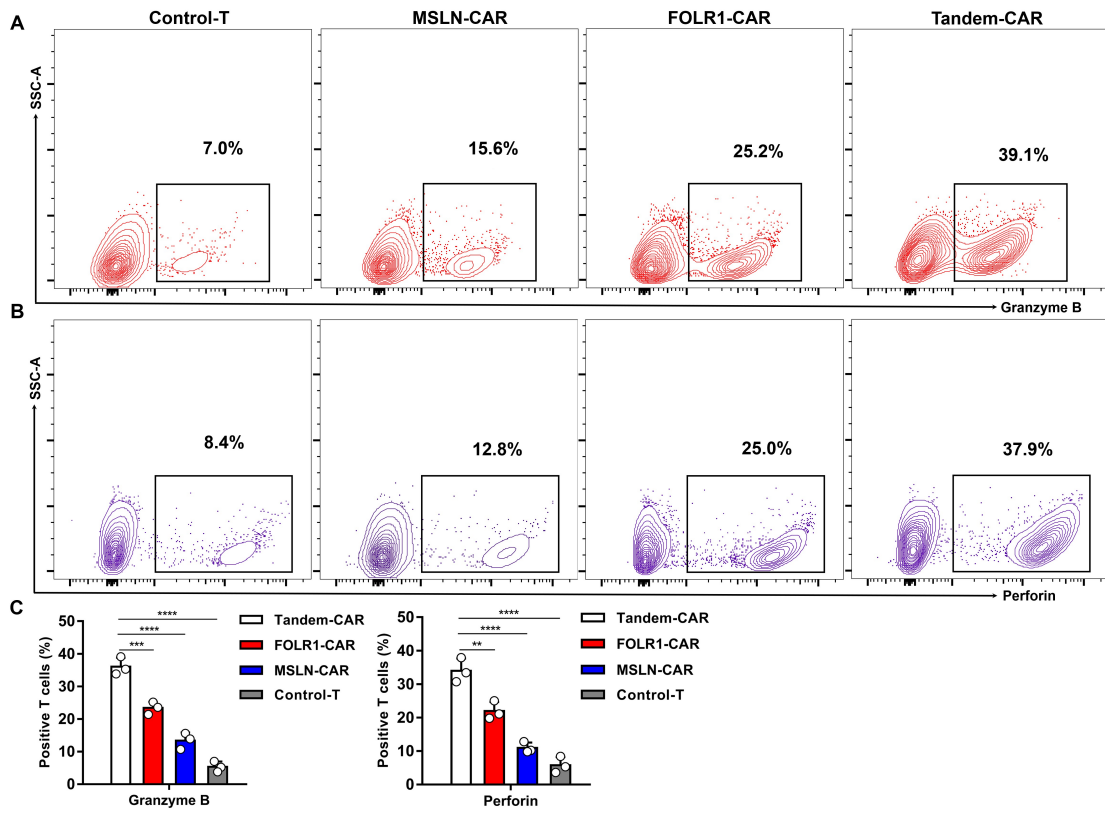
171 **(A, B)** Flow cytometric analysis of cell-surface CD4, CD8, CD62L, and CD45RO phenotypic

172 marker staining of Control-T cells and CAR-T cells after expansion. **(C)** The phenotype of CAR-T

173 cells was determined by measuring the percentages of CD62L⁺CD45RO⁺ central memory T cells

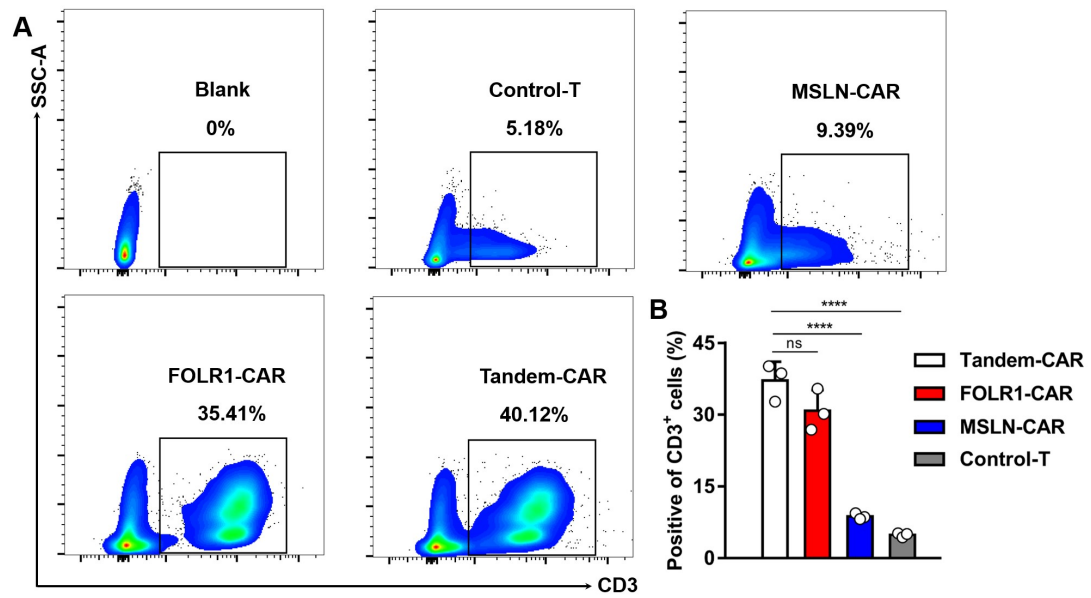
174 and CD62L⁻CD45RO⁺ effector T cells. Data are shown as the mean ± SD (n=3). ns: not

175 significant, * $P < 0.05$, and *** $P < 0.001$.



176

177 **Figure S2. Degranulation assay of different CAR-T cells. (A, B)** Flow cytometric analysis of
 178 degranulation levels of Control-T cells and CAR-T cells after incubation. **(C)** The data obtained
 179 for each group are compared in the histogram and shown as the mean \pm SD (n=3). $**P < 0.01$,
 180 $***P < 0.001$, and $****P < 0.0001$.



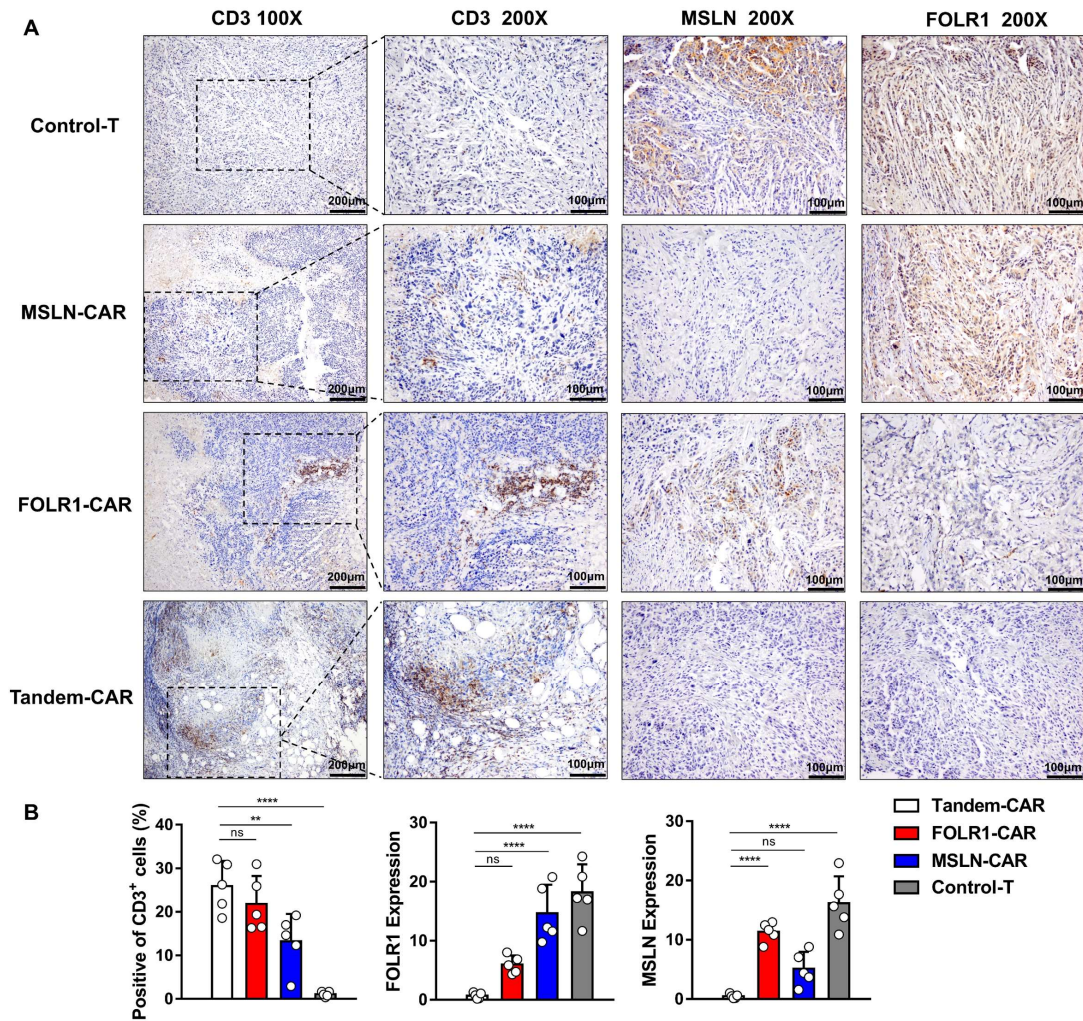
181

182 **Figure S3. Persistence of Tandem CAR-T cells *in vivo*.**

183 **(A)** The percentage of CD3-positive T cells in the peripheral blood was used to evaluate the

184 expansion of CAR T cells. **(B)** The data obtained for each mouse are compared in the histogram

185 and shown as the mean \pm SD (n=3). ns: not significant and **** $P < 0.0001$.



186

187 **Figure S4. Measurement of T cell infiltration and antigen expression levels after CAR-T cell**
 188 **therapy.**

189 **(A)** Representative photomicrographs of immunohistochemical staining. Paraffin tumor sections
 190 were stained with anti-human CD3 ϵ , FOLR1, and MSLN antibodies. **(B)** The statistical analysis is
 191 represented in the histogram, and the data are shown as the mean \pm SD (n=5). ns: not significant,
 192 $**P < 0.01$, and $****P < 0.0001$.

193 **References**

194 1. Tiraboschi C, Gentilini L, Velazquez C, Corapi E, Jaworski FM, Garcia Garcia JD, et al.
 195 Combining inhibition of galectin-3 with and before a therapeutic vaccination is critical for the
 196 prostate-tumor-free outcome. J Immunother Cancer. 2020;8(2).

197